Van Vleck paramagnetism of the trivalent Eu ions

Van Vleck paramagnetism of the trivalent Eu ions

Van Vleck paramagnetism of the trivalent Eu ions

Yusuke Takikawa, Shuji Ebisu, and Shoichi Nagata*
Department of Materials Science and Engineering, Muroran Institute of Technology,
27-1 Mizumoto-cho, Muroran, Hokkaido, 050-8585 Japan

Magnetic susceptibilities of Eu_2O_3, EuF_3 and $EuBO_3$ have been measured over the wide temperature range 5 to 650 K. The Van Vleck paramagnetism, with the ground state of $^7F_0$ ($S = 3$, $L = 3$), has been investigated comprehensively. The temperature independent paramagnetism emerges manifestly below approximately 100 K. The variation of the susceptibility with temperature for $EuBO_3$ is in satisfactory agreement with the coupling constant $\lambda = 471$ K, where the spin-orbit interaction is $\lambda \mathbf{L} \cdot \mathbf{S}$ for the Russell-Saunders coupling on the basis of Van Vleck theory with one parameter λ. The value of $\lambda = 490$ K can fit the susceptibility data of EuF_3. The deviation from the theory arises in Eu_2O_3. This discrepancy originates mainly from the influence of the crystalline field. Susceptibility of Gd_2O_3, having the ground state of $^8S_{7/2}$ ($S = 7/2$, $L = 0$), is also presented as a magnetic standard compound in comparison with these results.

PACS numbers:

I. INTRODUCTION

The rare earth Eu^{3+} ion has $4f^6$ electrons ($S = 3$, $L = 3$) which gives rises to seven energy levels, $^7F_0$, $^7F_1$, $^7F_2$, $^7F_3$, $^7F_4$, $^7F_5$, and $^7F_6$. The lowest ground state is $^7F_0$, which is not degenerate. Since the interval of the energy levels between the ground state $^7F_0$ and the successive first excited state $^7F_1$ is not large, but comparable with the thermal energy at the room temperatures. The levels of the multiplets are split by the spin-orbit interaction. The magnetic susceptibility of the majority for the rare earth ions satisfies the Curie's law, however europium and samarium ions are the exceptions because of the narrow energy separation. The most striking feature is that the temperature independent susceptibility arises in the low temperature region for Eu^{3+}. This type of the susceptibility is known as Van Vleck paramagnetism.[1]

The crystal structure of $EuBO_3$ has been extensively examined by Levin *et al.*[2] In this present study, the result of magnetic susceptibility of $EuBO_3$ will be clearly reported as a function of temperature over the wide range 5-650 K. Although the susceptibility of $EuBO_3$ was measured in the previous study, the temperature range was up to 300 K and the data are less accurate.[3] In order to compare the result of $EuBO_3$ with other trivalent europium compounds, the susceptibilities of Eu_2O_3[4–6] and EuF_3[7] have been re-investigated because the temperature range was not wide enough in the previous works and the analytical calculations were not sufficient to understand these results. The characteristic feature of the Van Vleck paramagnetism is that the temperature variation of the susceptibility can be analyzed by means of one-parameter.

We present the paramagnetic susceptibility of Gd_2O_3 as a magnetic standard compound with the ground state of $^8S_{7/2}$, $L = 0$. The susceptibility of Gd_2O_3 has been reported by previous researchers.[8–10]

The diamagnetic contribution to the susceptibility has been listed by Landolt-Börnstein.[11] We take the Pascal's additive law of these diamagnetic susceptibilities.

The estimated values are as follows: -3.8×10^{-5} emu per mole-f.u. for $1/2Gd_2O_3$, -3.8×10^{-5} emu per mole-f.u. for $1/2Eu_2O_3$, -5.3×10^{-5} emu per mole-f.u. for EuF_3, and -5.5×10^{-5} emu per mole-f.u. for $EuBO_3$. All the data will be presented below after these diamagnetic corrections, which are extremely small in comparison with the observed susceptibilities. We have performed a comprehensive investigation for the Van Vleck paramagnetism of the trivalent Eu ions.

II. THE VAN VLECK PARAMAGNETIC SUSCEPTIBILITY

Fig. 1 shows the lowest multiplet ^7F_J which consists of seven energy levels, where $^7F_0$ is the ground state. The number of f-electron of Eu^{3+} ion is 6 and the Hund rules give the spin quantum number $S = 3$ and the angular momentum $L = 3$. The spin-orbit interaction $\lambda \mathbf{L} \cdot \mathbf{S}$ with the coupling constant λ forms the energy levels in Russell-Saunders coupling. The energy E_J and the energy difference $E_J - E_{J-1}$ are given as

$$E_J = \frac{\lambda}{2}\{J(J + 1) - L(L + 1) - S(S + 1)\}, \quad (1)$$

$$E_J - E_{J-1} = \lambda J. \quad (2)$$

When the separation of the multiplet components is sufficiently large compared to $k_B T$, only the lowest energy is taken into consideration of the temperature variations of the physical properties. Nevertheless, for the comparable case with $k_B T$, the contribution of the different components should be included. The Zeeman Hamiltonian has the form

$$\mathcal{H}_{\text{Zeeman}} = -\boldsymbol{\mu} \cdot \mathbf{H} = \mu_B(\mathbf{L} + 2\mathbf{S}) \cdot \mathbf{H}. \quad (3)$$

$$J = 6 \quad {}^7F_6 \text{———————} E_6 = 21\lambda$$

$$J = 5 \quad {}^7F_5 \text{———————} E_5 = 15\lambda$$

$$J = 4 \quad {}^7F_4 \text{———————} E_4 = 10\lambda$$

$$J = 3 \quad {}^7F_3 \text{———————} E_3 = 6\lambda$$

$$J = 2 \quad {}^7F_2 \text{———————} E_2 = 3\lambda$$

$$J = 1 \quad {}^7F_1 \text{———————} E_1 = \lambda$$
$$J = 0 \quad {}^7F_0 \text{———————} E_0 = 0$$

$$\mathbf{Eu^{3+} \ 4f^6 \quad (S = 3, L = 3)}$$

FIG. 1: Energy levels of the lowest multiplet ${}^7F_J$ of trivalent Eu^{3+} ions in the absence of the external field. These separations are caused by the spin-orbit interaction $\lambda \mathbf{L \cdot S}$. The magnitude of λ indicates the energy difference between the ground state and the first excited state.

The paramagnetic susceptibility can be expressed using the Van Vleck theory,[1]

$$\chi_{para}(free \ Eu^{3+})$$

$$= \frac{\sum_{J=0}^{6} \chi_J (2J+1) e^{\frac{-E_J}{k_B T}}}{\sum_{J=0}^{6} (2J+1) e^{\frac{-E_J}{k_B T}}},$$

$$= N \frac{\sum_{J=0}^{6} [\frac{g^2 \mu_B^2 J(J+1)}{3k_B T} + \alpha_J](2J+1) e^{\frac{-E_J}{k_B T}}}{\sum_{J=0}^{6} (2J+1) e^{\frac{-E_J}{k_B T}}}. \tag{4}$$

Here N is the number of Eu^{3+} ion, k_B the Boltzmann constant, T the absolute temperature. The χ_J, the Lande's g-factor, α_J, and F_J are written, with the Bohr magneton μ_B, as

$$\chi_J = \frac{N g^2 \mu_B^2 J(J+1)}{3 k_B T} + N \alpha_J, \tag{5}$$

$$g = \frac{3}{2} + \frac{S(S+1) - L(L+1)}{2J(J+1)}, \tag{6}$$

$$\alpha_J = \frac{\mu_B^2}{6(2J+1)} \Big[\frac{F_{J+1}}{E_{J+1} - E_J} - \frac{F_J}{E_J - E_{J-1}} \Big], \tag{7}$$

$$F_J = \frac{[(L+S+1)^2 - J^2][J^2 - (S-L)^2]}{J}. \tag{8}$$

The explicit paramagnetic susceptibility of Eu^{3+} ions can be derived in the forms

$$\chi_{para}(free \ Eu^{3+})$$

$$= \frac{N\mu_B^2}{Z} \left(\frac{A}{3\lambda}\right), \tag{9}$$

$$Z = 1 + 3e^{\frac{-\lambda}{k_B T}} + 5e^{\frac{-3\lambda}{k_B T}} + 7e^{\frac{-6\lambda}{k_B T}}$$
$$+ 9e^{\frac{-10\lambda}{k_B T}} + 11e^{\frac{-15\lambda}{k_B T}} + 13e^{\frac{-21\lambda}{k_B T}}, \tag{10}$$

$$A = 24 + (13.5\frac{\lambda}{k_B T} - 1.5)e^{\frac{-\lambda}{k_B T}}$$
$$+ (67.5\frac{\lambda}{k_B T} - 2.5)e^{\frac{-3\lambda}{k_B T}}$$
$$+ (189\frac{\lambda}{k_B T} - 3.5)e^{\frac{-6\lambda}{k_B T}}$$
$$+ (405\frac{\lambda}{k_B T} - 4.5)e^{\frac{-10\lambda}{k_B T}}$$
$$+ (742.5\frac{\lambda}{k_B T} - 5.5)e^{\frac{-15\lambda}{k_B T}}$$
$$+ (1228.5\frac{\lambda}{k_B T} - 6.5)e^{\frac{-21\lambda}{k_B T}}. \tag{11}$$

Since the formulae of Eqs. (9)-(11) include only one unknown parameter λ, the value of λ can be determined uniquely in comparison with the experimental result of the temperature dependence of the susceptibility. In particular, the shift in the ground state energy is induced through the value of α_J. The α_J connects and mixes the
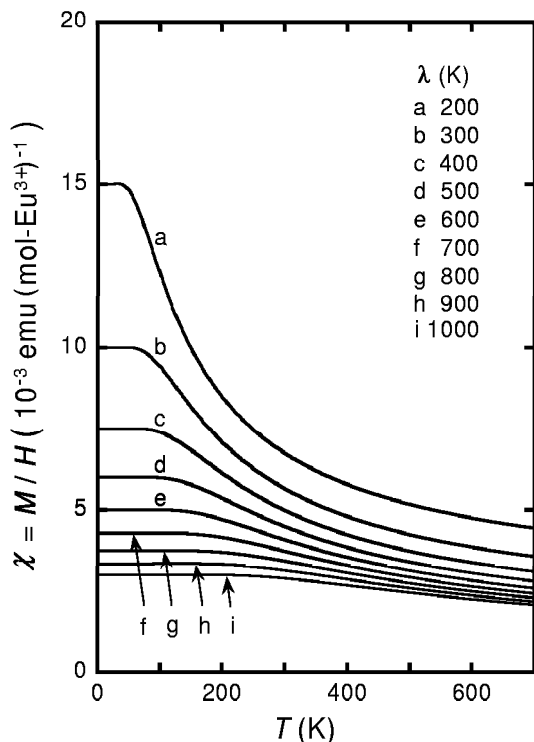
FIG. 2: Variation of the calculated magnetic susceptibility with the magnitude of λ for the energy levels shown in Fig. 1.

states between J and $J \pm 1$. The second-order perturbation correction produces this energy change in the ground state by the Zeeman energy from the excited states. Consequently the low lying excited state plays a significant role of the temperature independent susceptibility via the α_J, discussed below. It should be noted that the perturbing Hamiltonian is the Zeeman Hamiltonian itself and is given as Eq. (3).

Fig. 2 presents the calculated susceptibilities with the variation of λ as one parameter theory using Eq. (9). There is a characteristic feature as expected: the larger the value of λ, the higher is the beginning temperature below which the susceptibility becomes plateau, and furthermore the magnitude itself of the temperature independent susceptibility is lower. In other words, the higher the value of λ, the less is the hybridization from the excited state to non magnetic ground state, thus the value of the plateau becomes lower.

III. EXPERIMENTAL METHODS

The polycrystalline specimens $EuBO_3$ and Gd_2O_3 were prepared by a solid-state reaction. Mixtures of high-purity fine powders of Eu_2O_3 (99.99 %) and B_2O_3 (99.999 %) were heated to 1473 K in air and kept at this temperature for 3 hours, where 0.3 wt % excess B_2O_3 was added to compensate for possible volatility during heating. Subsequently, the sample $EuBO_3$ was quenched from 1473 K to the room temperature. The sample quality was not different from what was cooled down in the furnace after switching off the heating at 1473 K without the quenching. The prepared specimens with white in color were found to be stable under air after the synthesis. The specimens Eu_2O_3 (purity 99.99 %) and EuF_3 (99.9 %) used in this work were purchased from the Kishida Chemicals, Japan, which have extremely high purity. Impurity has not been detected for these three compounds within the X-ray measurements. The specimen of Gd_2O_3 was also prepared with the same method as $EuBO_3$, nevertheless the process of repeating was needed after regrind. The identification of the crystal structure and the determination of the lattice constants were carried out by X-ray diffraction for powdered specimen using Cu Kα radiation at room temperature.

The dc magnetizations of powder specimens in a constant magnetic field of 10 kOe were measured for all the specimens with a SQUID magnetometer (MPMS, Quantum Design Inc.) over the temperature range 5.0-650 K. The magnetic susceptibility is defined as $\chi = (M/H)$. Since the value of the susceptibility is low, then the demagnetizing field corrections have not been applied to any of our magnetic data.

IV. RESULTS AND DISCUSSION

A. Lattice constant

Fig. 3 indicates the X-ray powder diffraction profile of $EuBO_3$, which gives an evidence that $EuBO_3$ has the vaterite-type structure. The X-ray data have been analyzed assuming a hexagonal structure with the space group P6$_3$/mmc (no.194). The lattice constant, a, is obtained by the least square method. As far as we know, all the crystallographic data of the specimens which have been reported so far, are summarized in Table 1.[12] The specimens of the present work are specified in the symbols of (a), (f), (i), and (l) in Table 1.

B. Gd_2O_3

Fig. 4 represents the temperature dependence of the magnetic susceptibility $\chi = (M/H)$ for Gd_2O_3. The result obeys well the Curie-Weiss law. The value of effective Bohr magneton number p_{eff} Gd-ion^{-1} is extracted. The value of p_{eff} is obtained to be 7.79, which is close
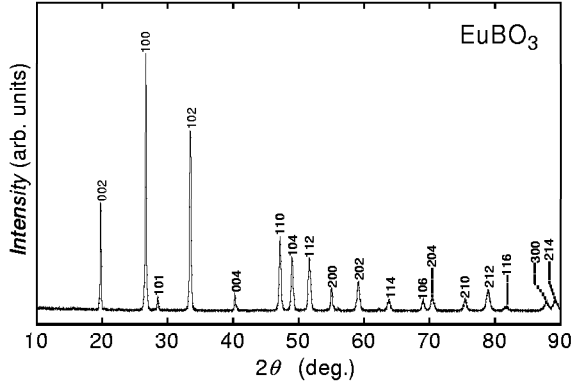
FIG. 3: X-ray powder diffraction pattern for EuBO₃ at room temperature.

FIG. 4: Temperature dependence of magnetic susceptibility $\chi = (M/H)$ of Gd_2O_3 and the inverse susceptibility $\chi^{-1} = (M/H)^{-1}$ in a constant magnetic field of 10 kOe. This specimen is considered as a standard material.

to the value of 7.94 as a free Gd^{3+} ion. The asymptotic Weiss temperature θ has a value of -14.6 K, reflecting the nature of antiferromagnetic exchange interaction.

C. Eu_2O_3, EuF_3 and $EuBO_3$

Fig. 5 shows the temperature variation of the susceptibility of Eu_2O_3 in $H = 10$ kOe. The plateau at low temperature is less pronounced, but increasing, which will be discussed below. Fig. 6 shows the susceptibility of EuF_3. The used specimens of Figs. 5 and 6 were extremely pure, but the inclusion of Eu^{2+} ions might be inevitable to preparation. The existence of small amount of Eu^{2+} ions as impurity can be detected below 15 K, reflecting the rapid increase in χ. Fig. 7 stands for the susceptibility of $EuBO_3$. As far as we know, the most typical and remarkable temperature independent paramagnetic susceptibility for Eu^{3+} ions has been now found at low temperatures.
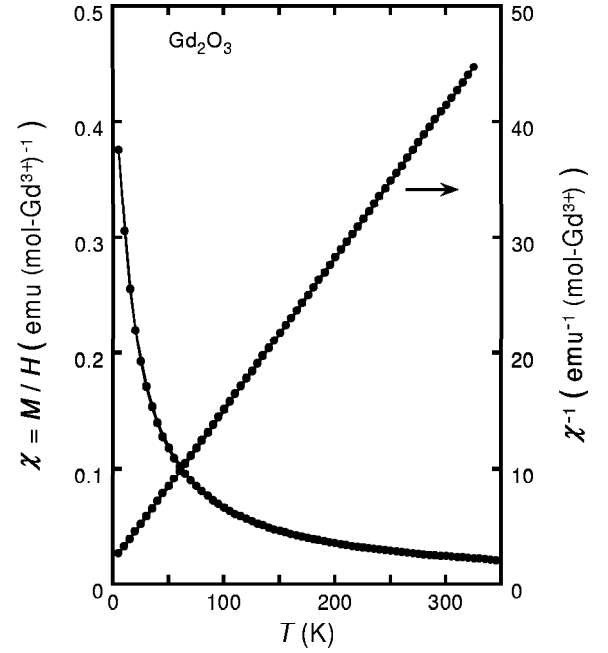
D. Comparison and analysis

Fig. 8 presents three susceptibilities for Eu_2O_3, EuF_3, and $EuBO_3$ in $H = 10$ kOe. The diamagnetic correction does not affect these magnitudes of the susceptibility as mentioned in the section of Introduction. In the first approximation, these three curves must coincide with each other with the same value of λ if these compounds would consist of sufficiently free paramagnetic Eu^{3+} ions. Next consideration is that these three compounds have been imposed on the individual different situation: intrinsically (a) influence of crystalline field, (b) magnetic anisotropy, and (c) extrinsically the foreign magnetic impurity such as Eu^{2+} ion.

Fig. 9 shows the enlargement of data at low temperature part below 150 K. Fig. 9 shows a manifest evidence of the existence of Eu^{2+} ions for Eu_2O_3 and EuF_3, because the rapid increase due to the Curie-like behavior below 15 K. The previous workers also have detected the similar increase for Eu_2O_3,[4] and EuF_3.[7] In experimental study for the susceptibility at low temperatures, it is im-
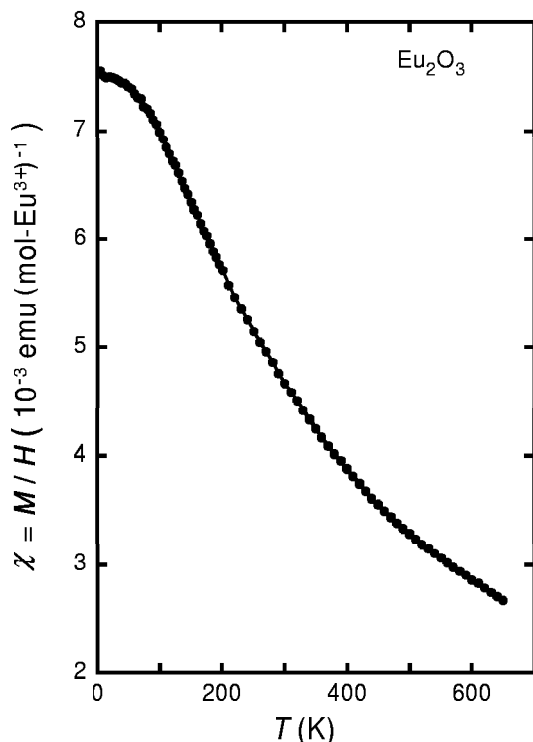
FIG. 5: Variation of the magnetic susceptibility with temperature for Eu_2O_3 in $H = 10$ kOe over the temperature region 5-650 K.
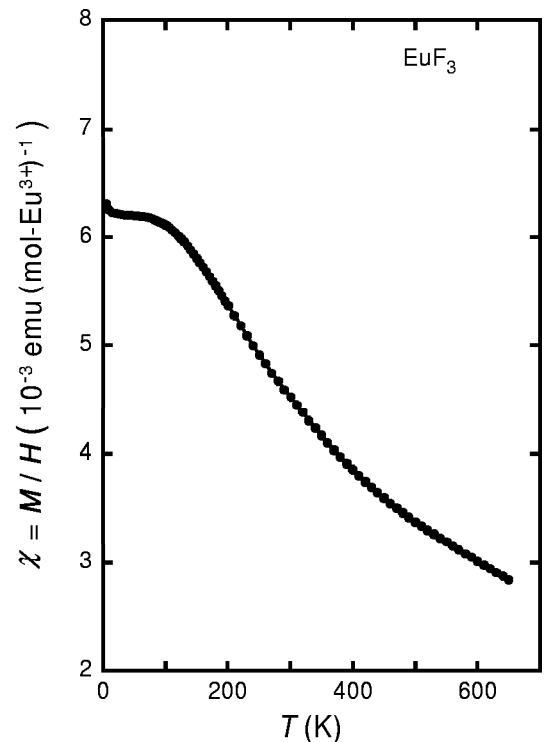
FIG. 6: Variation of the magnetic susceptibility with temperature for EuF_3 in $H = 10$ kOe. The sharp increase of the susceptibility below 15 K is presumably attributed to the existence of small amount of Eu^{2+} ions as impurity, which has strong Curie-like increase at low temperature.

portant to eliminate from the specimen even trace quantities of foreign paramagnetic impurities, because they can exhibit severely the Curie-like increase.

The Eu^{2+} ion is equivalent magnetically with Gd^{3+} ion, in which extremely large moment arises with $S = 7/2$. The valence mixing problem concerned with Eu^{2+} and Eu^{3+} is discussed, for example, in a Refs.[13,14]

Some Eu-based intermetallic compounds are known to have intermediate valence between Eu^{3+} (4f [6]) and Eu^{2+} (4f [7]) configurations. Valence fluctuations in Eu intermetallic compounds have attracted much attention because of the interest in hybridization between Eu^{2+} and Eu^{3+} ions for quantum mechanical mixing.[14] The intrinsic hybridization between Eu^{2+} and Eu^{3+} ions may take place in these intermetallic compounds. However, the present compounds of Eu_2O_3 and EuF_3 are not intermetallic, but are well defined ionic compounds. Therefore the possibility of the hybridization between Eu^{2+} and Eu^{3+} ions is exclusive.

We have carried out the estimation of the magnitude of the Curie contribution to the susceptibility for Eu_2O_3 and EuF_3. Our evaluation leads definitely that the number of Eu^{2+} ions does not exceed 0.01 percent in the two compounds.

Fig. 10 indicates the comparison with the theoretical prediction for Eu_2O_3. The discrepancy between the experiment and the theory cannot be attributed to the influence from the existence of the small amount of the Eu^{2+} ions.

Fig. 11 indicates the comparison with the theoretical prediction for EuF_3. The best fit of Eq. (9) to the experimental data gives the value of $\lambda = 490$ K. The susceptibility of EuF_3 has been studied in rather detail by Jayasankar et al.,[7] Our present experimental data are in good agreement with the reported data by them. They have taken into account the crystalline field even though the spin-orbit interaction is comparatively larger than crystalline field for lanthanides. It should be stressed that the fitting is in agreement sufficiently with Eq. (9) as seen in Fig. 11, without the influence from the crystalline field.

Fig. 12 indicates the comparison with the theoretical prediction for $EuBO_3$. The best fit of Eq. (9) to the experimental results leads to the value $\lambda = 471$ K. Now, the
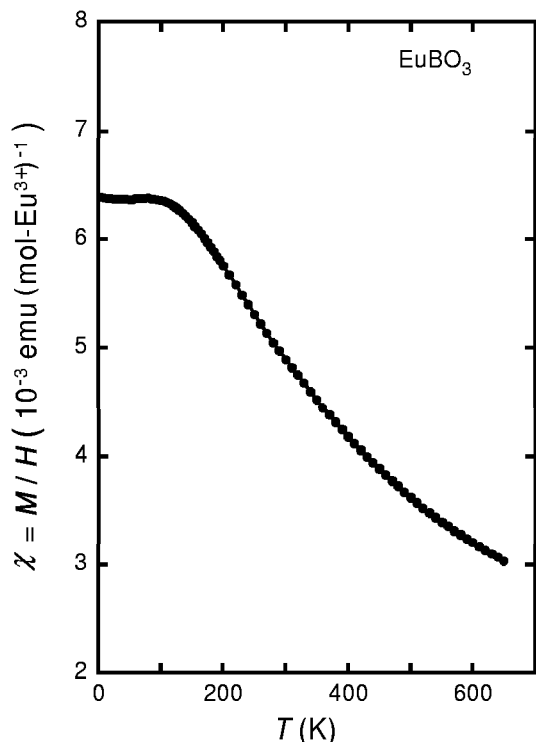
FIG. 7: Variation of the magnetic susceptibility with temperature for $EuBO_3$ in $H = 10$ kOe.

FIG. 8: Three magnetic susceptibilities below 300 K for Eu_2O_3, EuF_3, and $EuBO_3$. The $EuBO_3$ yields a plateau as a typical temperature independent susceptibility below 100 K.

wide temperature range observation has been performed up to 650 K. As can be seen in Fig. 12, however, the little deviation from Eq. (9) is appreciated, which is pronounced between 200-500 K. The experimental dada are slightly larger than that of expected value in Eq. (9).

E. Temperature-dependent effective moment

Since the excited state induces the magnetic combination to the ground state in the external magnetic field, the temperature independent permanent moment does not make sense for Eu^{3+} ion. Nevertheless the phenomenological temperature dependent effective Bohr magneton number is defined by the equation

$$p_{\mathrm{eff}} = \sqrt{\frac{3\chi k_B T}{N\mu_B^2}}. \tag{12}$$

Only when Curie's law is obeyed and is valid, the permanent moment p_{eff} is identified, therefore Eq. (12) is a simplified interpretation by means of a kind of artificial form. Here, the experimental values of p_{eff} through
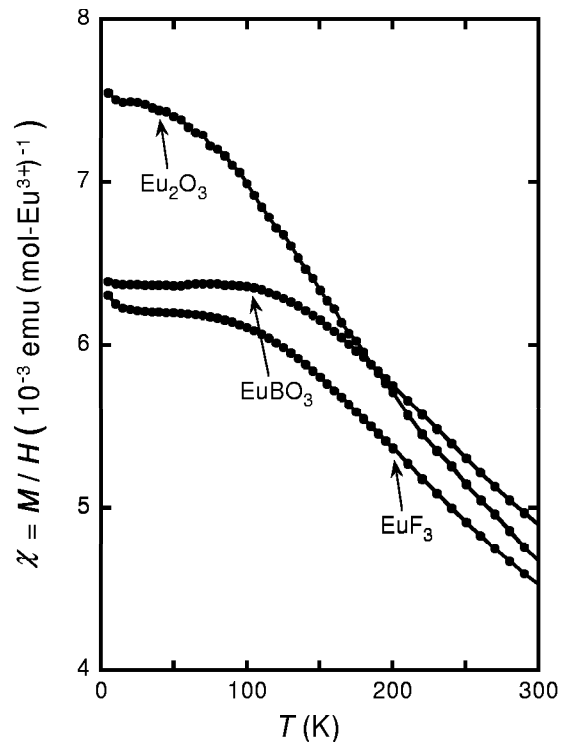
Eq. (12) are listed in Table 2 at only 300 K in order to compare them of the past bibliography.[1] These values of p_{eff} correspond with the moment induced by the Zeeman energy. It is noted that the p_{eff} approaches zero in Eq. (12) at $T = 0$ because χ is constant below 100 K and then p_{eff} is proportional to $\sqrt{T}$. However, this does not mean that the susceptibility χ of Eu^{3+} vanishes at absolute zero. The first term of Eq. (5) disappears when $J=0$ as in the component in Fig. 1, nevertheless the second term of $N\alpha_J$ becomes abnormally large. Thus, in the vicinity of $T = 0$, the susceptibility χ of Eu^{3+} is not zero.

F. Deviation from free ions in Eu_2O_3

Eq. (9) cannot fit very well the data of χ of Eu_2O_3. The appreciable deviation from the Van Vleck formula of Eq. (9) is seen in Fig. 10. On the other hand, the fittings of Eq. (9) to the data of EuF_3 (Fig. 11) and $EuBO_3$ (Fig. 12) are fairly good over wide temperature range. The comparison between Fig. 2 and Fig. 8 is interesting
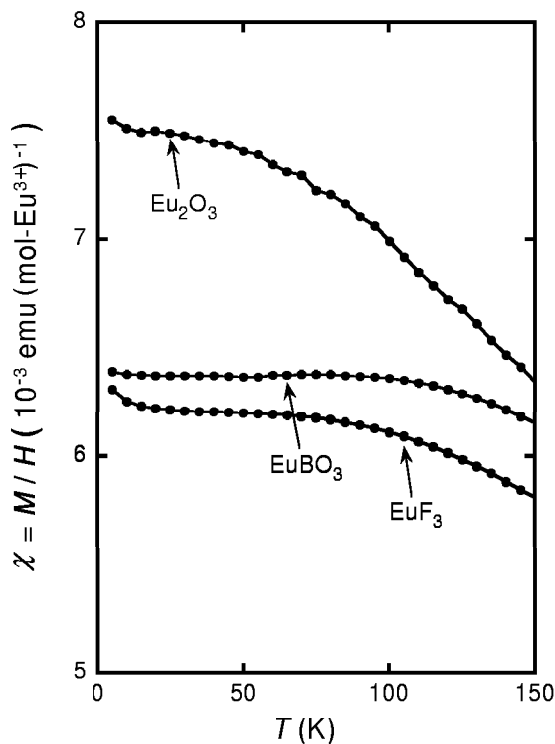
FIG. 9: An enlargement of data of Fig. 8. The Curie-like increase is seen below 15 K for Eu_2O_3 and EuF_3.

FIG. 10: Temperature dependence of χ for Eu_2O_3. The solid circles show experimental data and the three curves indicate calculated paramagnetic susceptibility for the values of λ. The data do not fit well the Eq. (9). Presumably the best fit would be given with $\lambda = 460$ K.

and instructive. The analysis of Fig. 2 indicates no-crossing in curves of χ each other with the variation of λ. Fig. 8 shows that χ of Eu_2O_3 crosses that of $EuBO_3$ around 180 K, and furthermore that of EuF_3 around 600 K. On the contrary, the temperature variations of EuF_3 and $EuBO_3$ have a reasonable difference without crossing in χ as seen in Fig. 8. The intrinsic mechanism to cause the deviation exists in Eu_2O_3. A plausible interpretation for this deviation should be required.

Possible origin of the deviation for Eu_2O_3 comes from the influence of the crystalline field. Table 3 proves compelling evidence for the rather strong influence of the crystalline field in Eu_2O_3 in comparison with EuF_3 and $EuBO_3$.[15] The bond length between Eu^{3+} and the O^{2-} ions is the shortest in Eu_2O_3. Eu^{3+} has two different sites of 1 and 2 and these bond lengths of Eu^{3+} - O^{2-} are shorter than those of EuF_3 and $EuBO_3$, as can be seen in Table 1. These crystal structure data might support the stronger influence from the crystalline field for Eu_2O_3.

The other indirect evidence is that the melting point of Eu_2O_3 is highest in the three compounds, reflecting the ionic bond is strongest and then the crystalline field could
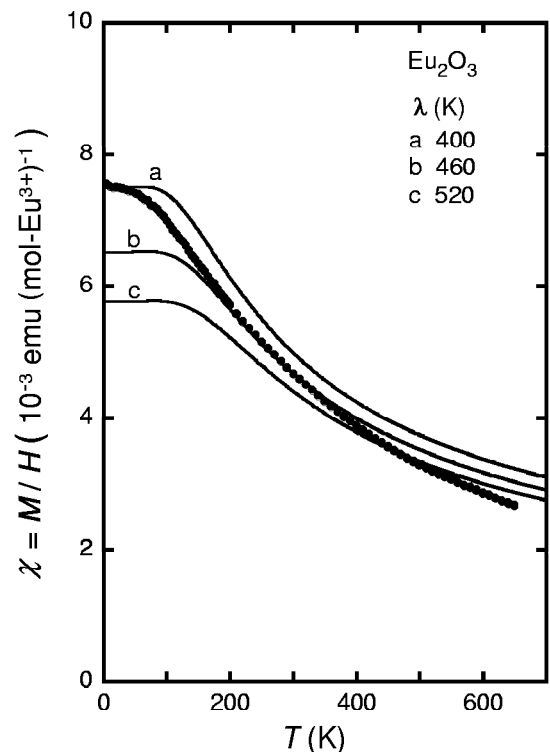
not be negligible. The detailed calculation of χ, taking into account of the crystalline field, has not been done in the present study because this is not main subject.

G. Higher-order corrections

A slight discrepancy is seen between the experimental and the calculated values over the temperature region 200-500 K in Fig. 12 for $EuBO_3$. The present analysis has confined to the original one parameter theory according to the theory of Van Vleck. Further detailed theoretical investigation for the rare-earth ions is available for understanding the result. The Russell-Saunders coupling might be incomplete, which have been provided by Judd.[16] The partial breakdown of the Russell-Saunders coupling is introduced and discussed in this theory. Unfortunately we cannot judge correctly the validity of this theory at the present. We do not discuss this problem in this paper.

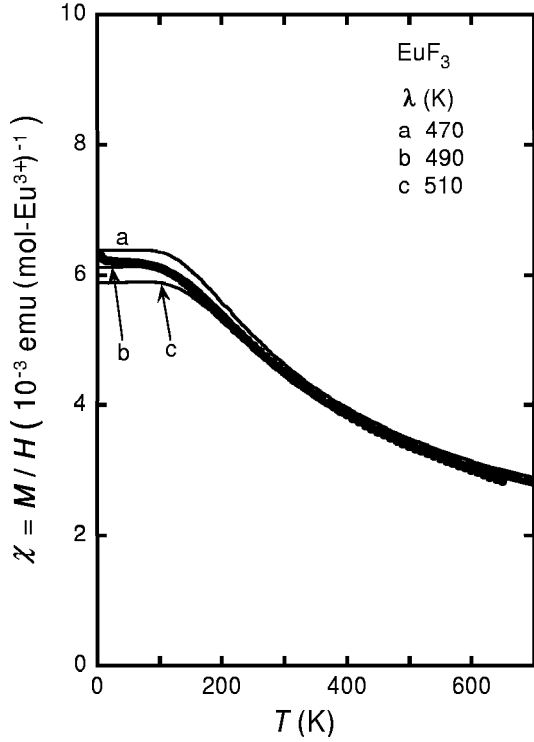There is another different approach to solve the seri-

FIG. 11: Temperature dependence of χ for EuF$_3$. The solid circles show experimental data and the solid curves indicate calculated χ for three values of λ. The best fit is given by λ = 490 K except the region below 20 K.
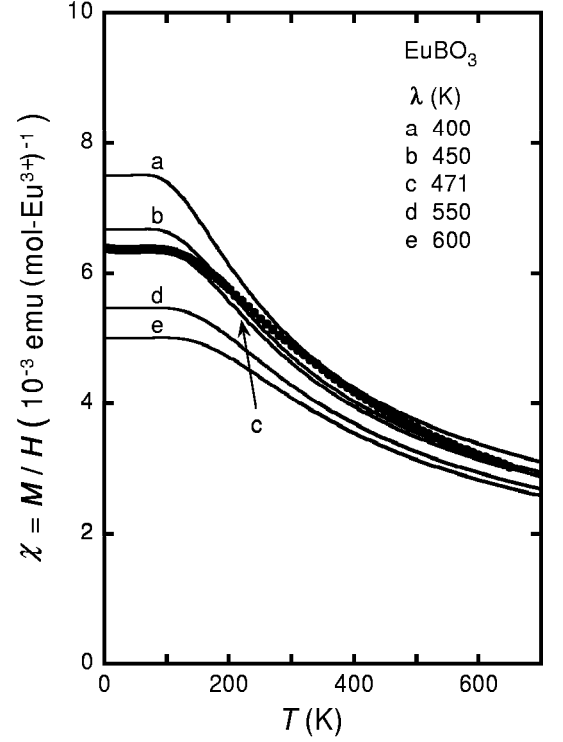
FIG. 12: Temperature dependence of χ for EuBO$_3$. Much emphasis is placed on the better fit to the low temperature data below 100 K. The results agree well with λ = 471 K using Eq. (9).

ous issue mentioned above. The higher order perturbation correction is the valuable tool of the theory. We have extended the formula of the magnetization to the third power of the field strength H. It is reasonable that the deviation should be attribute to the lacking of the higher-order corrections in the perturbation theory. This treatment can lead to the susceptibility depending on field of which strength is sufficiently large. The derivation have been carried out systematically by means of the perturbation theory, following the same procedure by Van Vleck.[1]

The energy level $E_{J,m}$ for each J in Fig. 1 is expressed as a power series in a field H of the form,

$$
\begin{aligned}
E_{J,m} &= E_J^{(0)} + H E_{J,m}^{(1)} + H^2 E_{J,m}^{(2)} + H^3 E_{J,m}^{(3)} \\
&+ H^4 E_{J,m}^{(4)} \cdots
\end{aligned}
\tag{13}
$$

Here the quantum number m specifies the degeneracy for $J > 1$. The $E_J^{(0)}$ is the energy in zero field and

$E_{J,m}^{(i)}$ is the i-th order small correction in the field from the perturbation by Zeeman energy.

The magnetic moment $(\mu_z)_{J,m}$ in the direction of the applied field is

$$
(\mu_z)_{J,m} = -\partial E_{J,m}/\partial H.
\tag{14}
$$

The magnetization M is given, using a Boltzmann distribution.

$$
M = N \frac{\sum_{J,m} (\mu_z)_{J,m} e^{\frac{-E_{J,m}}{k_B T}}}{\sum_{J,m} e^{\frac{-E_{J,m}}{k_B T}}}.
\tag{15}
$$

The final results can be written in the forms

$$
M = \frac{N}{Z} \sum_{J,m} [W_1 H + W_3 H^3] e^{\frac{-E_J^{(0)}}{k_B T}},
\tag{16}
$$

$$W_1 = \frac{\mid E_{J,m}^{(1)}\mid^2}{k_{\mathrm{B}}T} - 2E_{J,m}^{(2)}, \qquad (17)$$

$$W_3 = \frac{1}{k_{\mathrm{B}}T}(\ 2\mid E_{J,m}^{(2)}\mid^2 + 4E_{J,m}^{(1)}E_{J,m}^{(3)}\ )$$

$$-\frac{1}{(k_{\mathrm{B}}T)^2}(\ \mid E_{J,m}^{(1)}\mid^2 E_{J,m}^{(2)}\ )$$

$$+\frac{1}{(k_{\mathrm{B}}T)^3}\mid E_{J,m}^{(1)}\mid^4$$

$$-4E_{J,m}^{(4)}. \qquad (18)$$

It should be noticed that the magnetization does not have the second power of H, because it is an odd function of H without the residual magnetization in the absence of field. When the extension of the third power of magnetic field H is inclusive, the susceptibility depends on the field. The resultant form of Eq. (16) is applicable for all the rare earth ions, where N is the number of ions and the denominator Z is the partition function.

For example, the expressions of the first-order correction $E_{0,m}^{(1)}$ and the second-order correction $E_{0,m}^{(2)}$ (omitting the long expressions for $E_{0,m}^{(3)}$ and $E_{0,m}^{(4)}$) are given by using eigenfunctions,

$$E_{0,m}^{(1)} = \langle \psi_{0,m}\mid \mu_z \mid \psi_{0,m}\rangle, \qquad (19)$$

$$E_{0,m}^{(2)} = \frac{\sum\limits_{J,m}\mid\langle \psi_{0,m}\mid \mu_z \mid \psi_{J,m}\rangle\mid^2}{E_0 - E_J}, \qquad (20)$$

$$\mu_z = \mu_{\mathrm{B}}(\hat{L}_z + 2\hat{S}_z). \qquad (21)$$

If we take only the lowest term of W_1 in Eq. (16), then the Van Vleck formula of the susceptibility is obtained. Here the first term of $\mid E_{J,m}^{(1)}\mid^2/k_{\mathrm{B}}T$ in Eq. (17) corresponds to the first term of Eq. (5), and the second term of $-2E_{J,m}^{(2)}$ in Eq. (17) corresponds exactly to the α_J in Eq. (5). The temperature independent susceptibility of Eu^{3+} ions originates from the numerical value of 24 for the leading term in Eq. (11), which is caused by the correction of $E_{0,m}^{(2)}$. In this way, Eq. (4) to (11) are given without W_3H^3 term in Eq. (16).

The inclusion of W_3 term has been now formulated and established in the present study as Eq. (18) even though the calculation itself is extremely complicated. Unfortunately the actual calculations of the matrix elements for the higher-order corrections via W_3 term have never been made.

V. SUMMARY

In summary, a systematic study of the Van Vleck paramagnetism for Eu^{3+} ions has been carried out. The most typical temperature independent susceptibility at low temperatures has been demonstrated for the compound $EuBO_3$ with $\lambda = 471$ K.

* Author to whom correspondence should be addressed. Electronic address:
nagatas@almond.ocn.ne.jp(S.Nagata)
[1] J. H. Van Vleck, The Theory of Electric and Magnetic Susceptibilities, Oxford University Press, 1932, p. 226.
[2] E. M. Levin, R. S. Roth, and J. B. Martin, Am. Mineral. 46 (1961) 1030.
[3] Y. Laureiro, M. L. Veiga, F. Fernandez, R. Saez-Puche, A. Jerez, and C. Pico, J. Less-Common Met. 167 (1991) 387.
[4] A. S. Borovik-Romanov and N. M. Kreines, Sov. Phys. (JETP) 2 (1956) 657.
[5] R. V. Colvin, S. Arajs, and J. M. Peck, Phys. Rev. 122 (1961) 14.
[6] S. Arajs and R. V. Colvin, J. Appl. Phys. 35 (1964) 1181, and references therein.
[7] C. K. Jayasankar, E. Antic-Fidancev, M. L. Blaise, and P. Porcher, phys. stat. sol. (b) 133 (1985) 345.
[8] A. E. Miller, F. J. Jelinek, K. A. Gshneidner Jr., and B. C. Gerstein, J. Chem. Phys. 55 (1971) 2647.
[9] R. M. Moon and W. C. Koehler, Phys. Rev B 11 (1975) 1609.
[10] S. L. Bud'ko and P. C. Canfield, J. Mag. Mag. Mater. 299 (2006) 281.
[11] K.-H. Hellwege, A.M. Hellwege (Eds.), Landolt-Börnstein, New Series, Group II, vol. 16, Springer, Berlin, 1986, p. 402.

[12] (a) Present work; (b) D. Grier, G. MaCarthy, North Dakota State University, Fargo, North Dakota, USA, ICDD Grant-in-Aid, (1991); (c) Foex and Traverse, Hautes Temp. Refractaires 3 (1966) 429; (d) K. Martin, G. MaCarthy, North Dakota State University, Fargo, North Dakota, USA, ICDD Grant-in-Aid, (1990); (e) D. Grier, G. MaCarthy, North Dakota State University, Fargo, North Dakota, USA, ICDD Grant-in-Aid, (1991); (f) Present work; (g) Nat. Bur. Stand. (U.S) Monogr. 25 (1984) 20; (h) Nat. Bur. Stand. (U.S) Monogr. 25 (1983) 20; (i) Present work; (j) O.Greis, Private Communication, (1976); (k) O. Greis, Ph.D. Thesis, University of Freiburg I. Br. Germany (1976); (l) Present work; (m) E. M. Levin, R. S. Roth, and J. B. Martin, Am. Mineral. 46 (1961) 1030; (n) Y. Laureiro, M. L. Veiga, F. Fernandez, R. Saez-Puche, A. Jerez, and C. Pico, J. Less-Common Met. 167 (1991) 387.

[13] R. Stefani, A. D. Maia, E. E.S. Teotonio, M. A. F. Monteiro, M. C.F.C. Felinto, and H. F. Brito, J. Solid State Chem. 179 (2006) 1086.

[14] Y. H. Matsuda *et.al.*, J. Phys. Soc. Jpn. 77 (2008) 54713 and references therein.

[15] Eu_2O_3: S. Arajs and R. V. Colvin, J. Appl. Phys. 35 (1964) 1181; EuF_3: CRC Handbook of Chemistry and Physics, edited by David R. Lide, 89th edition, CRC Press, New York , 2008, pp. 4-63, and $EuBO_3$: E. M. Levin, R. S. Roth, and J. B. Martin, Am. Mineral. 46 (1961) 1030.

[16] B. R. Judd, Proc. Phys. Soc. (London), A 69 (1956) 157.

Table 1

Crystallographic data of the specimens [12].

Specimens		Crystal structure		
Gd$_2$O$_3$	a	Ia$\bar{3}$ (No.206) $a = 10.810$ Å	Cubic	
	b	Ia$\bar{3}$ (No.206) $a = 10.813$ Å	Cubic	
	c	$a = 3.86$ Å	Hexagonal $c = 6.16$ Å	
	d	C2/m (No.12) $a = 14.095$ Å	Monoclinic $b = 3.5765$ Å	$c = 8.7692$ Å
	e	C2/m (No.12) $a = 14.061$ Å	Monoclinic $b = 3.566$ Å	$c = 8.76$ Å
Eu$_2$O$_3$	f	Ia$\bar{3}$ (No.206) $a = 10.865$ Å	Cubic	
	g	Ia$\bar{3}$ (No.206) $a = 10.8683$ Å	Cubic	
	h	$a = 14.1126$ Å	Monoclinic $b = 3.6025$ Å	$c = 8.8089$ Å
EuF$_3$	i	Pnma (No.62) $a = 6.622$ Å	Orthorhombic $b = 7.020$ Å	$c = 4.398$ Å
	j	Pnma (No.62) $a = 6.6105$ Å	Orthorhombic $b = 7.0157$ Å	$c = 4.3959$ Å
	k	P$\bar{3}$c1 (No.165) $a = 6.9204$ Å	Hexagonal $c = 7.0856$ Å	
EuBO$_3$	l	P6$_3$/mmc (No.194) $a = 3.850$ Å	Hexagonal $c = 8.950$ Å	(Quenched specimen)
	m	$a = 3.845$ Å	Hexagonal $c = 8.94$ Å	
	n	P$\bar{6}$c2 (No.188) $a = 6.671$ Å	Hexagonal $c = 8.945$ Å	

The specimens of the present work are specified in (a), (f), (i), and (l).

Table 2

Effective magneton numbers p_{eff} at 300 K .

	χ 10^{-3} emu $(\text{mol-Eu}^{3+})^{-1}$	p_{eff}
Eu_2O_3	4.66	3.34
EuF_3	4.52	3.29
$EuBO_3$	4.89	3.43

Table 3

Bond length between Eu^{3+} and O^{2-} ions. The last column indicates the melting point.

	Space group	Bond	Bond length (Å)	Melting point (°C)
Eu_2O_3	$Ia\bar{3}$	Eu1 – O	2.309	1646
		Eu2 – O	2.330	
EuF_3	Pnma	Eu – F	2.333	1276
$EuBO_3$	P6$_3$/mmc	Eu – O	2.345	1540 ± 20